Applied Catalysis B: Environmental 244 (2019) 889–898

Contents lists available at ScienceDirect

Applied Catalysis B: Environmental

journal homepage: www.elsevier.com/locate/apcatb

Understanding the promoter effect of Cu and Cs over highly effective β-Mo_2C catalysts for the reverse water-gas shift reaction

Q. Zhang[a], L. Pastor-Pérez[a,b,*], W. Jin[a], S. Gu[a], T.R. Reina[a]

[a] Department of Chemical and Process Engineering, University of Surrey, Guildford, GU2 7XH, United Kingdom
[b] Laboratorio de Materiales Avanzados, Departamento de Química Inorgánica - Instituto Universitario de Materiales de Alicante Universidad de Alicante, Apartado 99, E-03080, Alicante, Spain

ARTICLE INFO

Keywords:
CO_2conversion
rWGS
Mo_2C catalyst
Cs promoter
Cu promoter

ABSTRACT

Mo_2C is an effective catalyst for chemical CO_2 upgrading via reverse water-gas shift (RWGS). In this work, we demonstrate that the activity and selectivity of this system can be boosted by the addition of promoters such as Cu and Cs. The addition of Cu incorporates extra active sites such as Cu^+ and Cu° which are essential for the reaction. Cs is an underexplored dopant whose marked electropositive character generates electronic perturbations on the catalyst's surface leading to enhanced catalytic performance. Also, the Cs-doped catalyst seems to be *in-situ* activated due to a re-carburization phenomenon which results in fairly stable catalysts for continuous operations. Overall, this work showcases a strategy to design highly efficient catalysts based on promoted β-Mo_2C for CO_2 recycling via RWGS.

1. Introduction

The excessive concentration of carbon dioxide (CO_2) in the atmosphere has been considered as one of the critical reasons for climate change and ocean acidification [1,2]. Consequently, capturing CO_2 and converting it into fuels and commodity chemicals have attracted numerous attentions. Reverse water-gas shift (RWGS) reaction (Eq. (1)) is a desired route for CO_2 utilization because the product of this reaction (syngas) can be used directly as feedstock in the Fischer-Tropsch process and further convert into fuels and chemicals.

$$CO_2 + H_2 \leftrightarrow CO + H_2O \ \Delta H^\circ\ 298\ K = +41\ kJ\ mol^{-1} \quad (1)$$

$$CO_2 + 4H_2 \leftrightarrow CH_4 + 2H_2O \ \Delta H^\circ\ 298\ K = -165\ kJ\ mol^{-1} \quad (2)$$

However, some factors such as high stability and low reactivity of CO_2 have to be considered in the chemical process [3]. Normally, a huge amount of heat is needed to produce CO. Besides, the reaction has a tendency to produce parallel unwanted products (Eq. (2)). In order to reduce the required energy and improve the selectivity of the RWGS reaction, exploring highly active, selective and stable catalysts is of significant demand. It is widely accepted that there are two main mechanisms for CO formation from RWGS reaction. One is a redox mechanism and the other is the formate decomposition mechanism. The catalysts used in RWGS reaction need to exhibit dual function in both these two mechanisms [4]. Typical RWGS catalysts consist of both a well dispersed active metal and metal-oxide support which can participate in the reaction [4,5]. Catalysts with such formulation have been studied extensively, such as Ni-CeO_2 [5], Cu-Al_2O_3 [6] and Pt/Al_2O_3 [7].

For the supports, Transition Metal Carbides (TMCs) seem to be appealing alternative supports because of their properties similar to precious metals. In addition, they are excellent substrates to disperse metallic particles [8,9]. In particular, previous studies have demonstrated that TMCs display high activity in olefin isomerization [10], WGS [11] and CO hydrogenation [12]. Among the available TMCs materials, molybdenum carbide (Mo_2C) was found to be itself (acting as an active phase) capable of activating the RWGS reaction via dissociating H_2 and scissoring C═O bond. Considering these properties and its low cost, Mo_2C has become one of the most promising support/active phase which can be employed in RWGS reaction.

Normally, molybdenum carbide has a variety of crystal structures, but it is commonly seen in two types, β-MoC_y (y = 0.5) with a hexagonal closed packed structure and α-MoC_{1-x} (x < 0.5) with a face-centered cubic (fcc) structure [13,14]. Both of these two types are active for the CO_2 hydrogenation. However, β-Mo_2C displays higher conversion of CO_2 since the Mo/C ratio of β-Mo_2C is higher than α-MoC_{1-x}. DFT calculation shows that the lower value the Mo/C ratio, the less C—O bonds are cleaved (when the ratio is equal to one, the MoC surface shows only chemisorption of CO_2 molecule without cleavage of the C—O bonds). Thermal carburization of hexagonal molybdenum

* Corresponding author at: Department of Chemical and Process Engineering, University of Surrey, Guildford, GU2 7XH, United Kingdom.
E-mail address: l.pastorperez@surrey.ac.uk (L. Pastor-Pérez).

https://doi.org/10.1016/j.apcatb.2018.12.023
Received 9 October 2018; Received in revised form 3 December 2018; Accepted 6 December 2018
Available online 07 December 2018
0926-3373/

carbide has been typically used to synthesize α-MoC_{1-x} and β-Mo_2C. In this process, methane is employed as carbon source and it seems that the formation of α-MoC_{1-x} requires higher methane concentration. Besides, after 20 h stability test in RWGS reaction at 600 °C, the α-MoC_{1-x} phase changes to β-phase indicating that the β-Mo_2C is more stable under the RWGS reaction conditions [15]. Seen from this perspective, β-Mo_2C is the right choice to conduct further modifications and improve its performance.

For the active phase, precious metals have been extensively studied due to its high activity such as Pt/CeO_2 [16], however, their elevated cost hinders the application for these materials. In order to overcome this problem, many studies have been carried out aiming to develop highly efficient and economically viable catalyst for the RWGS reaction. Cu-based catalysts have been widely used in this regard due to their high activity and selectivity. Previous studies demonstrate that Cu is a crucial active phase for the CO_2 hydrogenation in Cu-ZnO system when it is supported in a suitable oxide, such as CeO_2, Al_2O_3 or CrO_2. [17]. However, traditional Cu-based oxides catalysts suffer for poor stability due to the oxidation of the metallic Cu on the catalyst's surface [6] and the aggregation of the copper particles at high temperature [18]. In order to resolve this issue, Zhang et al. have used Mo_2C instead of oxides as the support material of the catalyst. This method effectively prevented high-temperature sintering on the surface of Cu-based catalyst since Mo_2C can considerably disperse and anchor the Cu particles over the substrate [19].

Alkali metals are also important promoters which can enhance CO_2 adsorption [20]. Among these alkali metals, Potassium and Rubidium are common promoters for producing alcohol in CO hydrogenation reactions [21,22]. Porosoff et al. synthesized a new potassium-promoted molybdenum carbide which is supported on γ-Al_2O_3 (K-Mo_2C/γ-Al_2O_3). Potassium helped Mo maintain in reduced phases that act as active sites in K-Mo_2C/γ-Al_2O_3. Since reduced Mo phases are significant for high selectivity towards CO and high catalyst stability, this catalyst exhibited high levels of activity in the RWGS reaction [23]. Comparing to potassium, studies dealing with Caesium are scarce despite its potential applicability as RWGS promoter [24]. Indeed, Caesium has bigger ionic radius than K and Na and therefore it is more prone to donate electrons creating electronic interactions that could favour the CO_2 hydrogenation process [23].

Under these premises, we have developed a series of novel multicomponent Cs-doped catalysts (Cs-Mo_2C, Cu-Cs-Mo_2C) for CO_2 conversion via RWGS reaction. The catalytic performance and the physicochemical properties of these two catalysts have been compared to reference materials (Cu-Mo_2C, β-Mo_2C and a commercial Mo_2C) and the main reasons for their excellent performance on the RWGS are carefully addressed.

2. Experimental section

2.1. Catalyst preparation

The β-Mo_2C catalyst was prepared by a TPC procedure described in the literature [19]. Ammonium paramolybdate ($(NH_4)_6Mo_7O_{24}{\cdot}4H_2O$, Sigma-Aldrich) was calcined to 500 °C at a heating rate of 5 °C/min and hold for 4 h to obtain MoO_3. This oxide precursor was sieved to retain particles with sizes between 200–400 μm. The powder was heated from room temperature (RT) to 300 °C at a heating rate of 5 °C/min under an atmosphere of 20% CH_4 and 80% H_2 and then the temperature was increased from 300 °C to 700 °C at a rate of 2 °C/min. The sample was treated in the above atmosphere at 700 °C for 2 h and then cooled to room temperature.

The oxide precursor of the Cs-Mo_2C catalyst was synthesized using a co-precipitation method. Ammonium paramolybdate ($(NH_4)_6Mo_7O_{24}{\cdot}4H_2O$, Sigma-Aldrich) was mixed with Cs_2CO_3 (Sigma-Aldrich) in distilled water (50 ml) at room temperature. The aqueous solution was stirred for 4 h and evaporated using a rotary evaporator at 75 °C, and dried at 110 °C overnight. Then the white powder was calcined at 500 °C for 4 h to obtain the Cs-MoO_3 precursor. After that, the same TPC procedure addressed above was used to prepare Cs-Mo_2C.

The same method was used for the synthesis of Cu-Mo_2C or Cu-Cs-Mo_2C catalyst using $Cu(NO_3)_2$ or $Cu(NO_3)_2$/Cs_2CO_3. For Cs-Mo_2C and Cu-Mo_2C, the content of the promoter elements was calculated to be 1 wt%. For Cu-Cs-Mo_2C, each content of the two elements was fixed at 1 wt%.

2.2. Catalyst characterization

X-ray photoelectron spectroscopy (XPS, K-ALPHA, Thermo Scientific) was used to analyse the surface chemistry of the prepared materials. All spectra were collected using Al-K radiation (1486.6 eV), monochromatized by a twin crystal monochromator, yielding a focused X-ray spot (elliptical in shape with a major axis length of 400 μm) at 3 mA × 12 kV. The alpha hemispherical analyser was operated in the constant energy mode with survey scan pass energies of 200 eV to measure the whole energy band and 50 eV in a narrow scan to selectively measure the particular elements. XPS depth profiles were obtained by sputtering the specimen with a 1 k eV Ar^+ ion beam. XPS data were analysed with Avantage software. A smart background function was used to approximate the experimental backgrounds and surface elemental composition were calculated from background-subtracted peak areas. Charge compensation was achieved with the system flood gun that provides low energy electrons and low energy argon ions from a single source.

The crystal structures of the samples were characterized by X-Ray Diffraction (XRD) analysis with an X'Pert Pro PANalytical at room temperature using Cu-K° (40 mA, 45 kV) over a 2 theta range of 10°-90°. X'PertHighscore Plus° was used to calculate the crystal sizes of the studied samples.

The textural characterization: The textural characterization of the catalysts was carried out by N_2 adsorption at −196 °C with an AUTOSORB-6 equipment (QUANTACHROME INSTRUMENTS). Samples were previously outgassed at 250 °C for 4 h.

2.3. Catalytic behaviour

The RWGS reactions were performed in a vertical continuous fixed bed reactor. The reactor was a 7 mm inner diameter quartz tube in which 0.25 g of catalyst (200–400 nm) was loaded on the quartz wool in the middle of the reactor. The sample was heated in the N_2 condition from room temperature to 400 °C. Then, the catalyst was exposed to the feed gas mixture of H_2:CO_2 = 4:1 at a constant weight hourly space velocity (WHSV) of 12,000 ml g^{-1} h^{-1}. For all the studied catalysts, tests were evaluated within a temperature range of 400 to 750 °C. At each temperature, the gas products were analysed after 10 min of steady-state reaction. An ABB AO2020 Advanced Optima Process Gas Analyser was used for the on-line analysis of reactants and products. In order to explore the effects of different H_2:CO_2 ratios on the performance of studied catalysts, reactions were tested at the same temperature and space velocity with a different H_2:CO_2 ratio of 4:1, 2:1 and 1:1. Stability tests were measured at a space velocity of 12,000g^{-1} h^{-1} with a H_2:CO_2 ratio of 4:1 at 550 °C for 50 h.

Performance of the catalysts was measured in terms of CO_2 conversion (Eq. (3)), CO selectivity (Eq. (4)) and CH_4 selectivity (Eq. (5)). The error in CO_2 conversion and CO/CH_4 selectivity for all the experiments was within ± 0.5%, as in previous work using this reaction set-up [24].

$$CO_2 \text{ conversion } (\%) = ([CO_2]_{In}\text{-}[CO_2]_{Out})/([CO_2]_{In}) \times 100 \quad (3)$$

$$CO \text{ selectivity } (\%) = ([CO]_{Out})/([CO_2]_{In} - [CO_2]_{Out}) \times 100 \quad (4)$$

$$CH_4 \text{ selectivity } (\%) = ([CH_4]_{Out})/([CO_2]_{In} - [CO_2]_{Out}) \times 100 \quad (5)$$

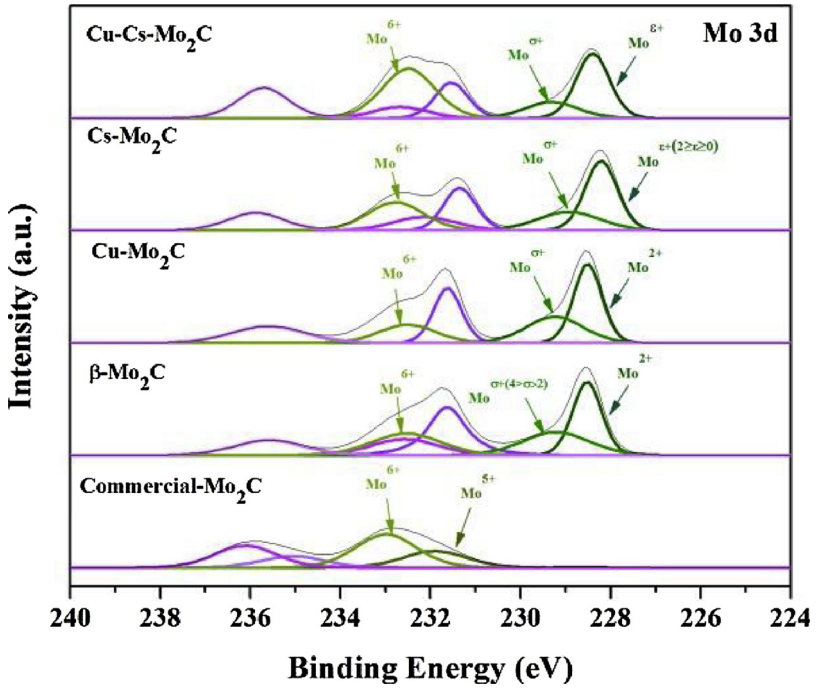

Fig. 1. X-ray photoelectron spectroscopy (XPS) Mo 3d spectra and the deconvoluted peaks of the β-Mo_2C, Cu-Mo_2C, Cs-Mo_2C, Cu-Cs-Mo_2C and commercial Mo_2C.

3. Result and discussion

3.1. Characterisation

3.1.1. XPS analysis

To investigate the electronic structures of all these five molybdenum carbides samples, Mo 3d XPS spectra were collected (Fig. 1 and Table 1). Mo 3d spectra are split into $3d_{5/2}$ and $3d_{3/2}$ peaks due to the spin-orbital coupling effect [25]. For the β-Mo_2C and Cu-Mo_2C catalysts, it is found that there are three species on molybdenum carbide surface. Doublets with $Mo3d_{5/2}$ peaks at 232.6 eV ± 0.2 eV are characteristic of Mo^{6+} which suggests the presence of single crystal MoO_3(010) [26–28]. The one with Mo $3d_{5/2}$ binding energy of 228.5 ± 0.1 eV is attributed to Mo^{2+} species involved in Mo-C bond [26,29–31] and another one with $3d_{5/2}$ binding energy of 229.3 ± 0.1 eV is identified as $Mo^{\sigma+}$ (where σ is the states between II and IV). Both $Mo^{\sigma+}$ and Mo^{6+} species are involved in Mo-O and Mo-O-C bonds as previously reported elsewhere [30,32,33].

Similar Mo 3d XPS spectra are observed for the Cs containing samples, including Cs-Mo_2C and Cu-Cs-Mo_2C. However, it should be noticed that the binding energy of the low valence state shifted to a lower binding energy when Cs is added as a dopant to molybdenum carbide, an effect observed for both Cu-Cs-Mo_2C and Cs-Mo_2C samples. The peaks located at 228.2 eV and 228.4 eV are assigned to $Mo^{\varepsilon+(0\le\varepsilon\le2)}$ since the binding energy of the species with these oxidation states are between 227.6 eV (Mo°) [29,34] and 228.5 eV (Mo^{2+}). This phenomenon is in accordance with XRD result which reveals strongly crystallized metallic Mo phase in the Cs-Mo_2C sample and in a lower extent, in the Cu-Cs-Mo_2C samples (Fig. 4). Interestingly, as shown in Table 1, $Mo^{\sigma+(2<\sigma<4)}$ is shifted to lower binding energy in Cs-Mo_2C in comparison to the other three catalysts. None of these catalysts was reduced or passivated prior to the XPS, but still, reduced metallic Mo appeared in the Cs containing samples. This can be explained as follows: Cs is an excellent electron donor with very low electronegativity. Therefore, in the Cs-Mo_2C sample, the electrons of Cs in Cs-Mo bonds are intensely attracted by Mo ions, leading to an increment of the electron charge density (ECD) around the Mo^{2+}. Hence the binding energies of Mo are shifted and the sample acquires a certain degree of metallic character. An analogous result in terms of the negative shift of Mo phase binding energy was recently reported when alkali metals such as K^+ was added to the Mo_2C/γ-Al_2O_3 based catalyst. According to the Bader charge analysis, potassium transferred almost one electron (Bader charge = 0.82e) to the surface of Mo_2C [23].

In the commercial Mo_2C catalyst, only the characteristic binding energies of Mo^{5+} $3d_{5/2}$ (231.9 eV) [29] and Mo^{6+} $3d_{5/2}$ (232.98 eV) were detected, which should respectively correspond to Mo_2O_5 and MoO_3 phases, indicating that commercial Mo_2C catalyst surface is completely oxidized and it is much difficult to be reduced than the other four catalysts.

The C1 s and O1 s spectra for Mo_2C-based catalysts are also shown in Fig. 2. For the C 1 s spectra (Fig. 2(A)), peaks at 283.5 ± 0.1 eV are assigned to carbidic carbons in Mo_2C [35]. It can be seen that no carbidic carbon was detected on the surface of the commercial Mo_2C catalyst, which is in accordance with Mo XPS spectra, indicating that

Table 1
$Mo3d_{5/2}$ binding energies of all samples.

Sample	$Mo3d_{5/2}$(eV)					$Cu2p_{3/2}$			$Cs2d_{5/2}$	Cu/Mo (at/at)	Cs/Mo (at/at)
	$Mo^{\varepsilon+(0\le\varepsilon\le2)}$	Mo^{2+}	$Mo^{\sigma+(2<\sigma<4)}$	Mo^{5+}	Mo^{6+}	$Cu^{0,1}$	$Cu(OH)_2$	CuO	Cs^{1+}		
Commercial Mo_2C	–	–	–	231.9	233.0	–	–	–	–		
β-Mo_2C	–	228.5	229.2	–	232.5	–	–	–	–		
Cu-Mo_2C	–	228.5	229.2	–	232.5	932.3	935.0	–	–	0.048	
Cs-Mo_2C	228.2	–	228.9	–	232.8	–	–	–	724.4		0.215
Cu-Cs-Mo_2C	228.4	–	229.3	–	232.5	932.1	934.9	941.7(944.1)	724.1	0.131	0.115

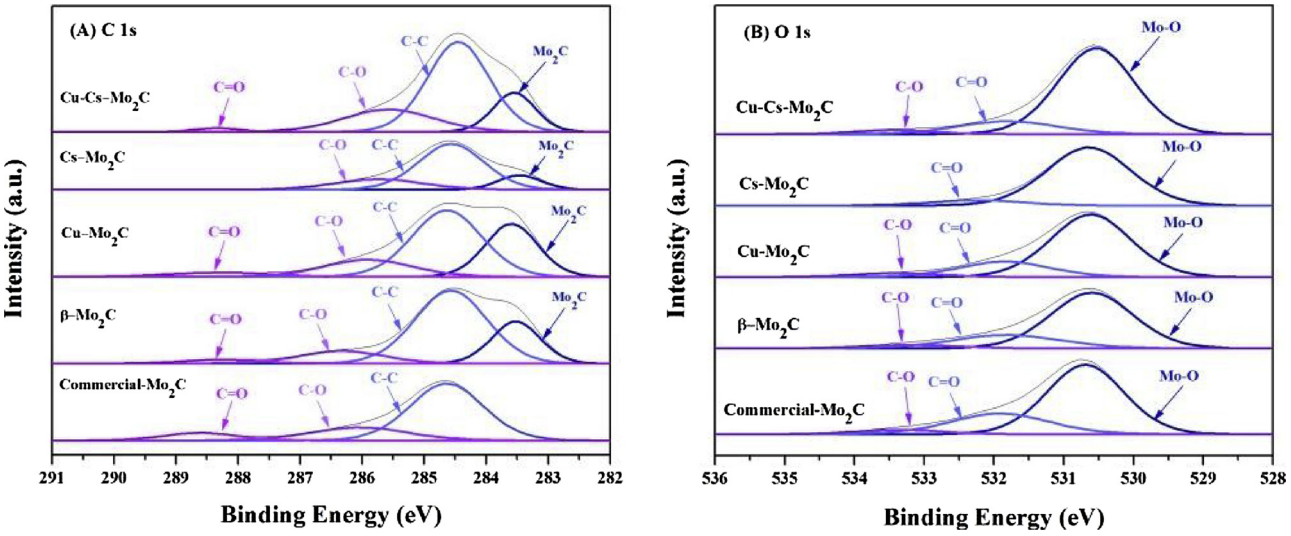

Fig. 2. (A) C 1 s and (B) O 1 s XPS spectra of all catalysts.

the Mo_2C on the surface of catalyst was completely oxidized. The major peaks at 284.6 ± 0.1 eV are identified as the surface C—C bonds belonging to graphitic carbon [28,34]. The peaks at 286 ± 0.6 eV and 288.4 ± 0.4 eV are assigned to species containing C–O and C═O bonds, respectively. These can be associated with carbonates and formates on the catalyst surface due to traces of contamination [32,36,37].

As for the O1 s spectra, two different species are present on the surface of the Mo_2C-base catalyst. The binding energy of O 1 s located at 530.7 ± 0.1 eV is assigned to the oxygen in MoOx formulations. Peaks at 532 ± 0.2 eV are indicative of strongly bound O = C and peaks at 533.4 ± 0.1 eV are ascribed to O-C [37].

The surface chemical state of Cu and Cs was also analysed (Fig. 3). Cu $2p_{3/2}$ XPS spectra for the Cu-containing samples show that the peaks at 932.2 ± 0.1 eV dominate the spectrum, which should be assigned to Cu^{1+} (Cu_2O) and Cu° (metallic Cu). It is difficult to distinguish these two valence state in XPS since Cu° (932.3 ± 0.1 0.1 eV) present a similar binding energy to that of Cu_2O (932.4 ± 0.2 eV) [38,39]. Peaks at 934.9 ± 0.1 eV are attributed to Cu^{2+} species in $Cu(OH)_2$ [40]. For the Cs 3d spectra, the binding energy of Cs $3d_{5/2}$ located at 724.2 ± 0.2 eV is univocally identified as Cs^+ [41].

For Cu-Mo_2C, Cu^+ and metallic Cu are the main Cu species on the surface of catalysts. However, with the addition of Cs to the Cu-Mo_2C, two peaks located at 941.66 eV and 944.13 eV were detected, indicating that the copper species may interact with molybdenum carbide and partially evolve from Cu° to Cu^+ to Cu^{2+} (CuO) [40,42]. In parallel and when compared to Cs-Mo_2C, the binding energy of Cs $3d_{5/2}$ in Cu-Cs-Mo_2C shifted from 724.4 eV to 724.1 eV. This once again reflects the electronic interactions in our multicomponent catalysts indicating an electronic transfer from Cu° and Cu^+ to Mo with caesium acting as a bridge, to facilitate electronic transfers.

Since the different Cu species have an important impact on the catalytic performance and it is hard to distinguish between Cu^+ and Cu° in a typical XPS experiment, Cu LMM Auger electron spectroscopy (AES) was collected to differentiate these two species more precisely. As shown in Fig. 3(C) and (D), AES spectra exhibit the coexistence of Cu^+ and Cu° in the two samples. The proportion of Cu° is roughly 60% and the percentage of Cu^+ is approximately 40% in the Cu-Mo_2C sample. As for the Cs promoted system, the proportion of Cu° is (42%). This is in accordance with our previous discussion showing that there is an electronic interaction Cu-Cs-Mo in such a way that copper transfers electronic density through Cs to Mo and partially evolves towards from Cu° to Cu^+ in the Cu-Cs-Mo_2C sample.

3.1.2. XRD analysis

Fig. 4(A) shows the XRD patterns of the fresh catalysts. The XRD patterns of the spent catalysts after RWGS reaction are also shown for comparison (Fig. 4(B)). The peaks at 2Θ of 34.4°, 38°, 39.4°, 52.1°, 61.5°, 69.6° and 74.6° are attributed to the diffraction features of β-Mo_2C with hexagonal closet packing (HCP) crystal structure (β-Mo_2C, JCPDS 35-0787) [43,44] while the peaks at 40.6 and 58.7 are assigned to metallic Mo (JCPDS 42-1120) [45]. It seems that Mo phase appears only in the samples containing Cs. Ryoichi Kojima et al. confirm that if Cs is added to MoO_3 before the carburization, Mo metal will be formed to partially replace β-Mo_2C [46]. As a good electron donor, Cs transferred electrons to Mo in the catalyst and stabilised Mo reduced phases ($Mo^{\varepsilon+(0\leq\varepsilon\leq2)}$) in good agreement with our XPS data. This result suggests that the Cs has a reduction effect on the molybdenum carbide catalysts. No peaks were observed for MoO_2 [34,47] or MoO_3 [48], indicating successful bulk carburization of the Mo oxides precursors. There is no obvious copper or caesium peaks for the Cu-Mo_2C, Cs-Mo_2C and Cs-Cu-Mo_2C, pointing out that copper and caesium have particle sizes smaller than the detection limit (4 nm).

The main crystallite sizes of these fresh and spent samples were calculated using the Scherrer equation as presented in Table 2. Prior to the reaction, the Mo_2C crystallite size of the commercial Mo_2C sample is 105.5 nm. To reduce the size of Mo_2C sample, a TPC procedure has been used to synthesize β-Mo_2C. The TPC procedure was fairly successful resulting in a crystallite size of 16.5 nm for the pure β-Mo_2C. Therefore, the TPC method was selected for the rest of the catalysts synthesis. The addition of Cu to the oxide precursor MoO_3 barely affect the crystallite size of the Cu-Mo_2C with just a slight increase (18.3 nm). The size of Cs-Mo_2C is 33.8 nm, two times bigger than the size of β-Mo_2C. More remarkable is the expansion of the carbide lattice when Cu and Cs are added simultaneously to oxide precursor (MoO_3) resulting in a crystallite size of 168.8 nm.

Changes in the particle size after the reaction are worth mentioning. As showcased in Table 2, the Mo_2C crystallite size in the commercial Mo_2C, β-Mo_2C, Cs-Mo_2C and Cu-Mo_2C catalysts had small particle size increments compared to their fresh counterparts. However, for Cu-Cs-Mo_2C, the most interesting observation is the absence of Mo peaks after the RWGS reaction (not even in the form of Mo oxides). Similarly, the crystallite size of Mo peak in Cs-Mo_2C decreased from 169.4 nm to 77 nm after the reaction. It is suggested that the RWGS reaction had a re-carburization effect on the catalysts. Metallic Mo has been carburized to Mo_2C and the crystallite size of Mo_2C peak in Cu-Cs-Mo_2C was also affected by the reaction atmosphere, which decreased from 168.8 nm to 32.5 nm accounting for the re-carburization effect.

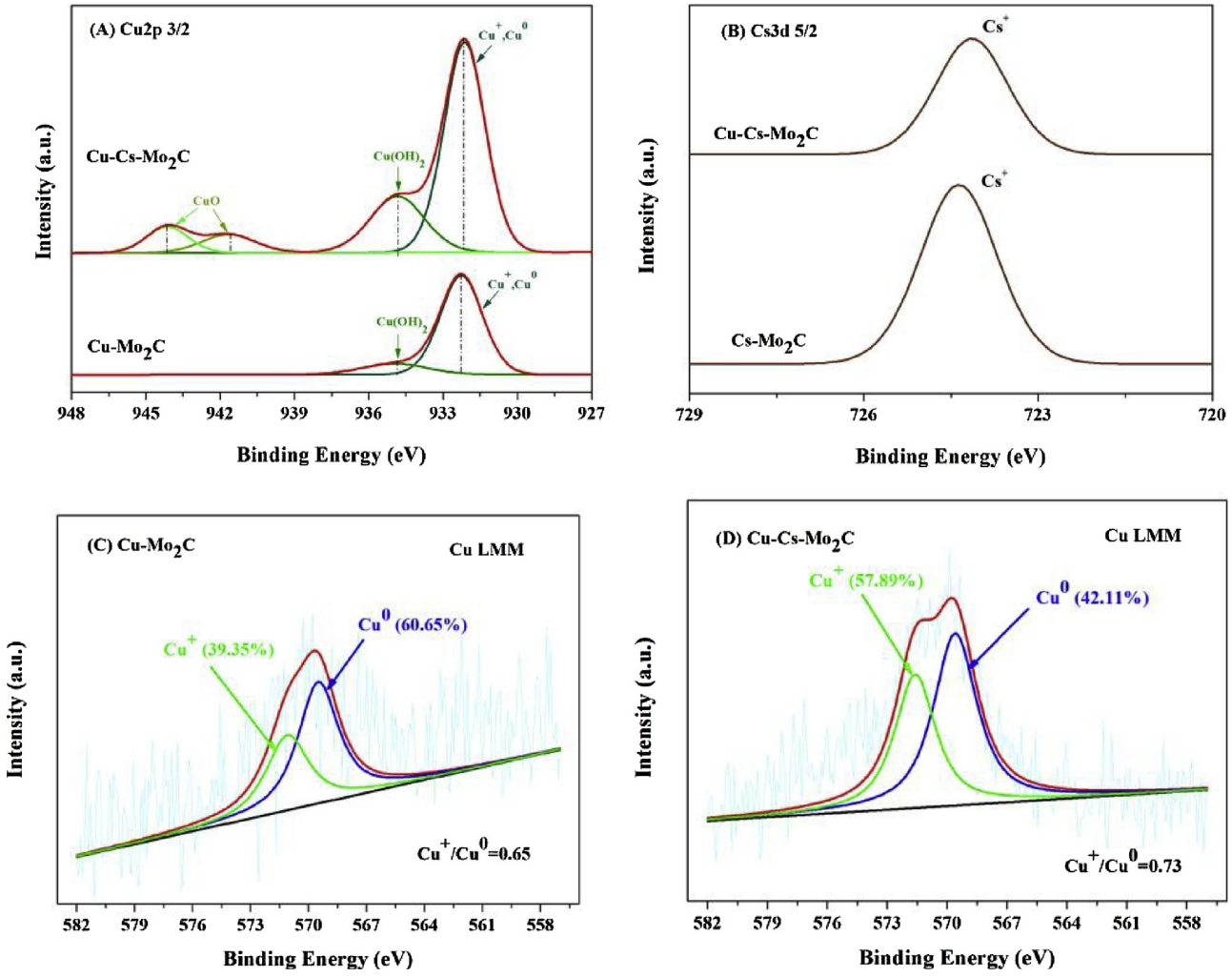

Fig. 3. (A) Cu $2p_{3/2}$ XPS spectra of the Cu-containing samples (B) $Cs3d_{5/2}$ XPS spectra of the Cs-containing samples (C) Cu LMM AES spectra of Cu-Mo_2C (D) Cu LMM AES spectra of Cu-Cs-Mo_2C.

3.1.3. Textural properties analysis

The N_2 adsorption-desorption isotherms for the fresh samples are shown in Fig. 5 and the BET surface area, pore volume and pore size of these Mo_2C samples are summarized in Table 3. According to the IUPAC standard, the isotherms of all the samples exhibit a typical type-IV curve with a pronounced capillary condensation step, characteristic of mesoporous materials [49,50].

The surface area of β-Mo_2C reached at 9 m^2/g, twice the value of

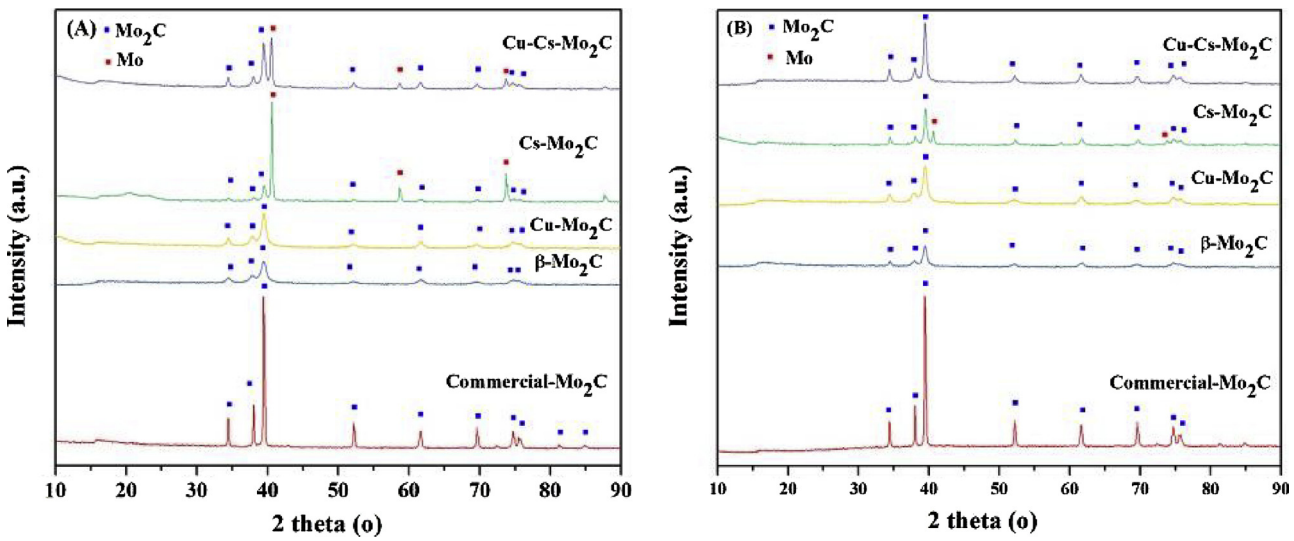

Fig. 4. X-ray diffraction patterns for the β-Mo_2C, Cu-Mo_2C, Cs-Mo_2C, Cu-Cs-Mo_2C and commercial Mo_2C. A) Fresh samples B) Post reaction samples.

Table 2
XRD crystallite size for both fresh and post reaction catalysts.

Catalyst crystallite sizes(nm)[1]	Fresh		Post Reaction	
	Mo_2C	Mo	Mo_2C	Mo
Commercial Mo_2C	105.5		120.6	–
β-Mo_2C	16.5		21.6	–
Cu-Mo_2C	18.3		22.2	–
Cs-Mo_2C	33.8	169.4	38.4	77
Cu-Cs-Mo_2C	168.8	92	32.5	–

[1] Estimated using Scherrer equation.

Table 3
Textural properties of the studied catalysts.

Catalyst	Surface Area[a] (m^2/g)	Pore Volume[b] (cm^3/g)	Pore size[c] (nm)
Commercial Mo_2C	4	0.005	3.4
β-Mo_2C	9	0.020	3.8
Cu-Mo_2C	10	0.023	3.8
Cs-Mo_2C	7	0.015	2.4
Cu-Cs-Mo_2C	8	0.019	1.9

[a] calculated by the BET equation.
[b] Pore volumes calculated from the N_2 desorption at a relative pressure of 0.96.
[c] BJH desorption average pore diameter.

commercial Mo_2C (4 m^2/g). The addition of Cu is shown to slightly increase the surface area of β-Mo_2C. The pore volume and pore size of the Cu-Mo_2C are nearly identical to β-Mo_2C. This result confirms that the surface area is not the determining factor in the RWGS reaction.

However, the data in Table 3 reveal that the surface areas, pore volumes and pore sizes all decreased when Cs was added to these samples. This phenomenon could be attributed to a partial blockage of these mesoporous of the carbide support.

3.2. Catalytic performance

3.2.1. Catalytic activity & selectivity

Fig. 6 depicts the CO_2 conversion and CO/CH_4 selectivity for the RWGS reaction over the studied catalysts. It can be seen that the commercial Mo_2C is active for RWGS reaction with the activity increasing upon rising up the temperature. All the homemade Mo_2C catalysts display considerably higher activities than the commercial one. This result could be ascribed mainly to the severe surface oxidation of the commercial Mo_2C whose surface according to the XPS analysis is dominated by Mo^{5+} and Mo^{6+} species. Indeed the XPS spectra (Figs. 1 and 2(A)) show the absence of Mo_2C species in the surface of the commercial catalyst. Compared to the commercial one, the other four catalysts exhibit higher resistance to oxidation and preserve an electronically richer surface which helps to activate CO_2.

Among the synthesised catalysts, Cu-containing materials and β-Mo_2C catalyst show very similar conversion levels. However, in terms of the selectivity, Cu-Mo_2C has higher selectivity to CO than that of β-Mo_2C and Cu-Cs-Mo_2C. Very likely the chemical state of Cu in our catalysts plays a key role to explain the activity/CO selectivity trends. The Cu-Mo_2C sample presents Cu^{2+} species in the XPS spectra which population increased notably on the surface of Cu-Cs-Mo_2C (Fig. 3.A). Considering that the RWGS reaction is more favoured on metallic copper than on oxidized copper [51] the marked presence of Cu^{2+} species on the multicomponent Cu-Cs-Mo_2C catalysts explains its poorer CO selectivity when compared to Cu-Mo_2C. The latter correlates fairly well with the simplified redox mechanism of the RWGS reaction mediated by Cu catalysts shown below:

$$CO_2 + 2Cu^{\circ} \rightarrow Cu_2O + CO \quad (6)$$

$$H_2 + Cu_2O \rightarrow H_2O + Cu^{\circ} \quad (7)$$

In this simplified mechanism, Cu° provides the active sites to dissociate CO_2 and the role of Cu^{+} is to stabilize the intermediate formate species when the formate mechanism prevails over the redox or takes place simultaneously [6]. In any case, the richer concentration of Cu^{2+} species on the Cu-Cs-Mo_2C surface accounts for its poorer CO selectivity.

The conversion of the RWGS reaction over Cs-Mo_2C is lower than the other three homemade materials, likely due to the largest block by caesium of Mo active sites. However, in terms of CO selectivity, Cs-Mo_2C is the best catalysts in the low-temperature range reaching 100% CO selectivity in the temperature window 400–500 °C, an excellent result for a potential integration with a Fischer-Tropsch reactor whose

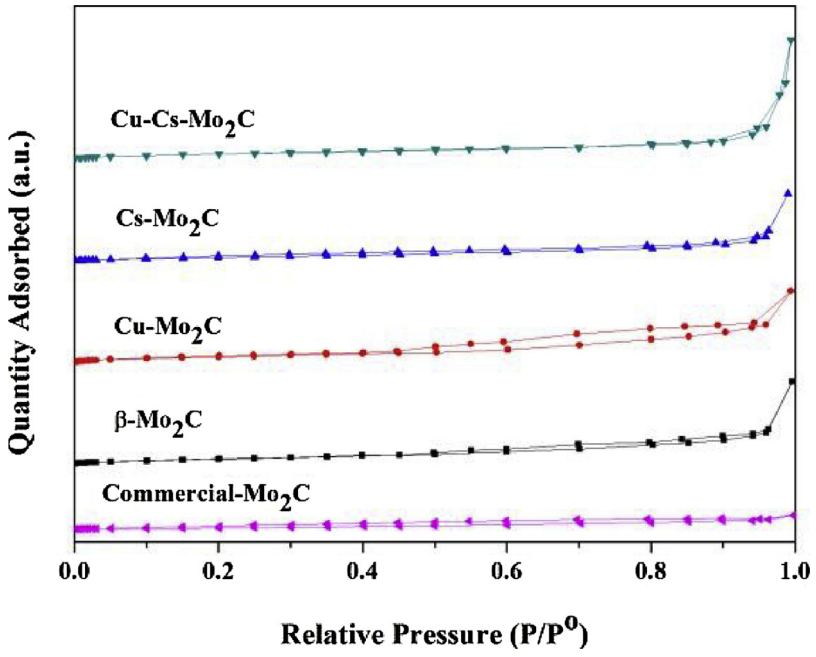

Fig. 5. N_2 adsorption-desorption of all fresh catalysts.

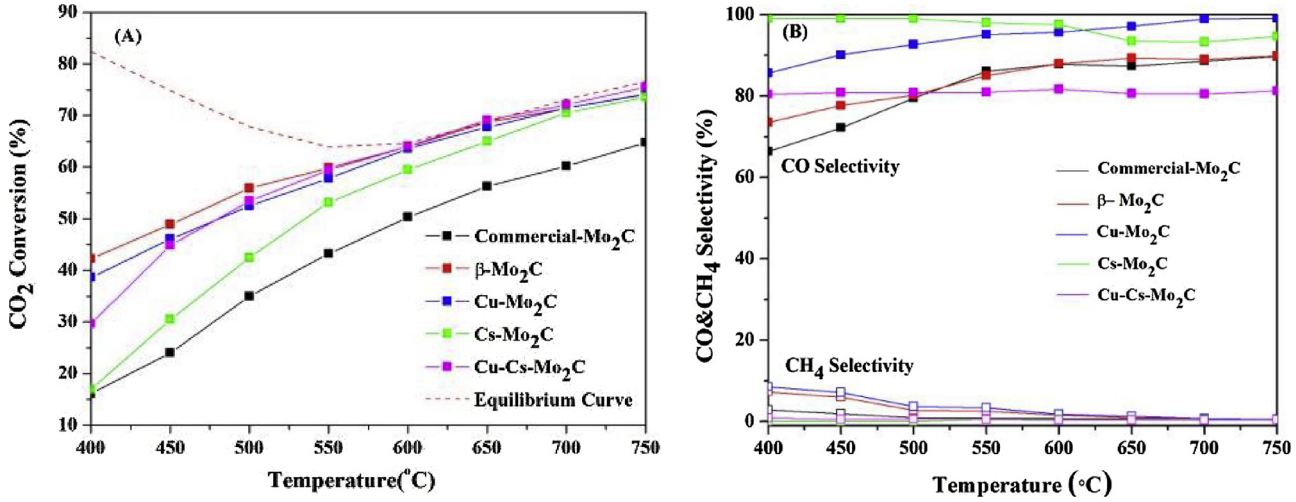

Fig. 6. (A) CO_2 conversion (B) CO and CH_4 selectivity for the β-Mo_2C, Cu-Mo_2C, Cs-Mo_2C, Cu-Cs-Mo_2C and commercial Mo_2C.

operational temperatures are lower than those of the RWGS units. The excellent selectivity of the Cs-Mo_2C could be attributed to the electronic effects of Cs on Mo_2C. As shown in XPS spectra, Mo binding energies are shifted towards lower values in Cs-Mo_2C indicating a charge transfer from Cs to Mo_2C. Porosoff et al. have demonstrated that the addition of K can enhance CO_2 adsorption (both chemisorption and physisorption) and reduce CO_2 dissociation barrier through transferring electrons to Mo_2C [23]. In our case, Cs also transfers electrons to the surface of Mo_2C leading to metallic-like Mo species in good agreement with our XPS and XRD data. Therefore, the positive charge (Cs-cation) increases the dipole-dipole interaction during the CO_2 physisorption thus increasing the physisorption energy. Meanwhile, the negatively charged molybdenum surface facilitates the activation of CO_2 (by transforming the molecule from a linear to bent configuration) and drives the selectivity towards CO. Indeed, as shown in the graph the selectivity of CO over Cs-Mo_2C is boosted and as a partial conclusion, it seems that CO_2 conversion is associated to Mo_2C phases while the enhanced selectivity maybe related to Mo metallic-like particles.

Typically, molybdenum carbide catalysts have passivation problems since carbide surfaces are very reactive. Freshly prepared Mo_2C catalysts are partially oxidised when exposed to air, so they are normally passivated by 1% O_2/ He mixture to avoid violent oxidation. After the passivation treatment, the Mo_2C has an oxidised surface with a variety of Mo species with oxidation states between + IV and + VI, which is more thermodynamically stable in air [52]. However, passivation is not always beneficial to the catalysts' performance. *Nagai et al.* showed that passivation of molybdenum carbide with dilute O_2 reduced its activity for CO_2 hydrogenation to form CO and CH_4 [53]. Besides, *Heng Shou et al.* confirm that alkali metal can reduce the sensitivity of the catalyst to passivation by 1% O_2. The passivation of unpromoted Mo_2C/Al_2O_3 decreased the overall activity of the catalyst, whereas passivation of Rb promoted Mo_2C/Al_2O_3 did not significantly influence the activity [54]. In our case, Cs has been used as a promoter to maintain Mo in low valence and diminish the impact of passivation. Indeed, bearing in mind a realistic process the suppression of the passivation step involves substantial operating cost savings. For the equilibrium curve, both methanation and RWGS reaction have been considered during the simulation process. The thermodynamic equilibrium curves provided in Fig. 6 mirror the natural competition methanation/RWGS. In the low-temperature range, high CO_2 conversion could be achieved via methanation. At the high-temperature range, the RWGS becomes the dominant process and the equilibrium CO_2 conversion levels increase upon incrementing the temperature. Since our catalysts are very selective towards RWGS the experimental CO_2 conversion values observed along the whole studied temperature range reflect mainly the effect of the reverse shift process; in other words, the CO_2 conversion always increases with temperature.

Overall, all the studied catalysts present an excellent activity/selectivity balance and certainly outperform the behaviour of a commercial Mo_2C. Also, it must be highlighted that the samples do not require any pre-treatment prior to the reaction thus avoiding extra steps (and cost) in a potential implementation of these catalysts in a real CO_2 conversion unit. Among the studied series Cu-Mo_2C resulted to be the most active material but in terms of selectivity, Cs-Mo_2C is the most interesting system especially when an integrated process with a syngas upgrading unit is considered. Therefore this catalyst was selected for further catalytic tests.

3.2.2. *Influence of H_2:CO_2 ratio*

Considering the cost of hydrogen it would be interesting to develop a RWGS catalyst able to run effectively at relatively low H_2:CO_2 ratios [55]. In this sense, we have studied the influence of this parameter on the RWGS reaction performance conserving the same WHSV (12,000 ml g^{-1} h^{-1}). As shown in Fig. 7(A), the CO_2 conversion of the RWGS reaction over Cs-Mo_2C is notably affected by the hydrogen concentration in the reactor inlet. It seems clear that CO_2 conversion is favoured at high H_2:CO_2 ratios. According to the reaction stoichiometry, RWGS reaction should be successfully accomplished for H_2:CO_2 ratio of 1.0. The fact that higher hydrogen concentrations favour the process could be related to adsorptions capacity and hydrogen coverage on catalysts surface. The preferential adsorption of CO_2 on the surface could result in a CO_2-rich surface for hydrogen-poor reaction mixtures and therefore fewer chances for the reactants to interact. This situation is alleviated when the partial pressure of hydrogen is increased. In fact, the observed trend regarding the influence of the H_2:CO_2 also reflects the thermodynamics of the reaction. In terms of CO selectivity (Fig. 7(B)), it can be observed that for these three H_2:CO_2 ratios the CO selectivity remained constant at 100% at a temperature of 400 °C and 450 °C. However, the selectivity of CO decreased with temperature, indicating that CO selectivity over Cs-Mo_2C is favoured at low temperatures – again pointing its suitability to couple the RWGS unit with a lower temperature reactor. It is interesting to note that in the high-temperature range from 600 °C onwards the CO selectivity is enhanced for H_2:CO_2 ratio 1:1.

3.2.3. *Stability study*

Long-term runs are essential for any realistic application and in particular for CO_2 conversion units where a continuous CO_2 effluent has to be treated. In this sense, the Cs-Mo_2C catalyst was subjected to a long-term stability run of about 50 h and its performance compared to that of the β-Mo_2C. As shown in Fig. 6, Cs-Mo_2C exhibits a high CO

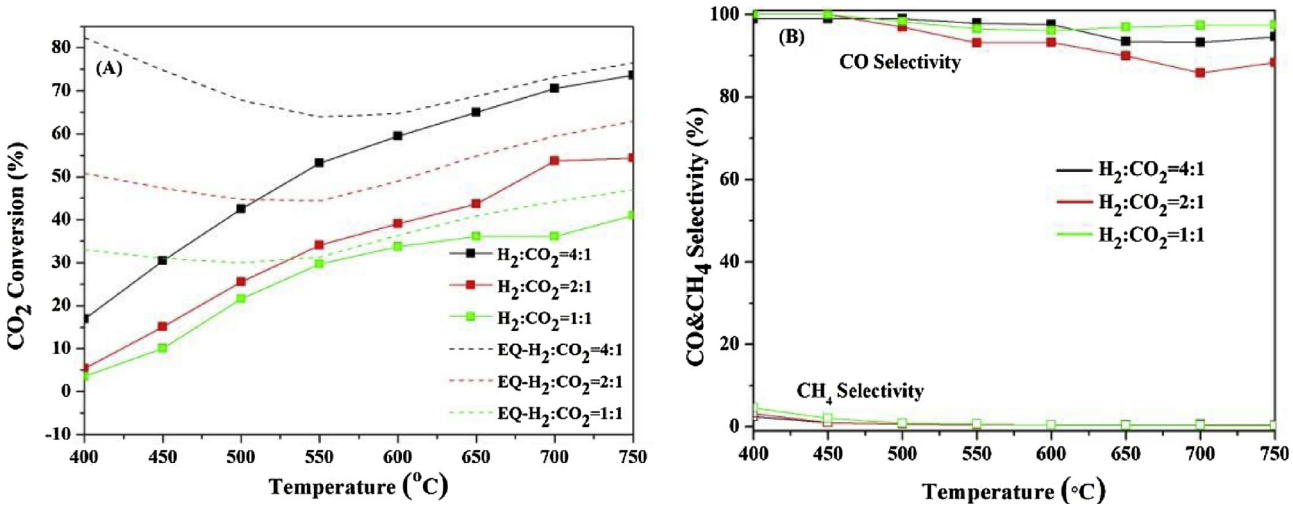

Fig. 7. CO_2 conversion (A) and CO&CH_4 selectivity (B) for Cs-Mo_2C at H_2:CO_2 ratio of 4:1, 2:1, 1:1.

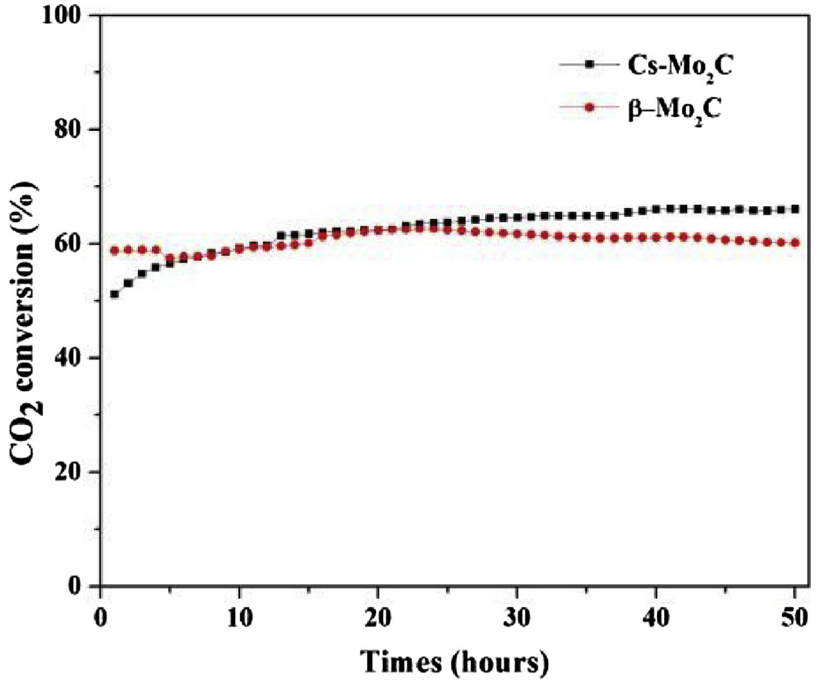

Fig. 8. Stability test at 550 °C, WHSV of 12,000 ml g^{-1} h^{-1} with a H_2:CO_2 ratio of 4:1 for Cs-Mo_2C and β-Mo_2C.

selectivity and a relatively high CO_2 conversion at 550 °C. Thus, the condition of WHSV = 12,000 ml g^{-1} h^{-1} with a H_2:CO_2 ratio of 4:1 at 550 °C was chosen for this test which results are depicted in Fig. 8.

In general terms, both catalysts exhibit fairly stable performance after 50 h of continuous operation. For the β-Mo_2C, CO_2 conversion remains approximately constant at 60%. On the other hand, the Cs-Mo_2C shows a better catalytic activity after the 5 h stability test. The conversion of RWGS reaction over Cs-Mo_2C increased from 54.8% to 60% after 12 h test and came up to 66% after 50 h test. This in-situ activation is just a confirmation of the re-carburization process for Cs-Mo_2C during the RWGS in good agreement with our XRD observations. As shown in Fig. 4(B), Mo metal peaks of Cs-Mo_2C catalyst are weaker than those of the fresh catalyst. The crystallite size of Mo peak in Cs-Mo_2C decreased from 169.4 nm to 77 nm after the reaction (Table 2), indicating that metallic Mo has been carburized to Mo_2C. In addition to the re-carburisation, the formation of smaller Mo clusters (electronically rich due to the electron donation from Cs) also accounts for this apparent in-situ activation effect. Along with the excellent stability the Cs-doped catalysts maintained 98% of selectivity towards CO a higher selectivity outcome compared to that of the unpromoted β-Mo_2C. In other words, the Cs-Mo_2C catalyst is a promising system for chemical CO_2 recycling in the gas phase via RWGS able to perform steadily for long-term runs.

4. Conclusion

This work reflects the potential of Mo_2C based catalysts for chemical CO_2 recycling via RWGS. The addition of promoters such as Cs and Cu have a remarkable positive impact on the catalytic performance – enhanced activity/selectivity. The surface chemistry of the promoted catalysts seems to play a major role to account for the beneficial effect of the promoters. The presence of Cu^+ and Cu° species in the Cu-Mo_2C favours the RWGS reaction. As for the Cs promoted material, the electropositive character of Cs facilitates the electronic transfer from Cs to Mo and leads to an electronically rich surface which favours the selectivity towards CO. Indeed, the Cs-promoted catalyst reaches 100%

CO selectivity in the low-temperature range which makes this catalyst a promising system for the integration of RWGS and syngas gas upgrading unit which typically runs at lower temperatures than the shift reactor.

Our work also showcases the fact that relatively high H_2:CO ratios are needed to achieve higher CO_2 conversions in the RWGS reaction under the studied conditions. Overall, the CO_2 conversion decreases when the H_2:CO ratio goes from 4 to 1 with no remarkable effects on the selectivity. As for the catalysts' stability, our long-term run reveals that both the β-Mo_2C and the Cs-Mo_2C are very robust catalysts exhibiting excellent stability with no apparent deactivation. Interestingly, Cs-Mo_2C is in-situ activated during RWGS due to a re-carburization process along with the electronic transfer from Cs to Mo favoured under the reaction conditions. Also, the catalysts developed in this work do not require any kind of pre-treatment prior to the reaction resulting advantageous for the potential implementation of these catalysts in a real CO_2 conversion unit. Overall, this work represents an approach towards the design of efficient promoted-Mo_2C catalysts for the RWGS with potential applications in gas phase CO_2 upgrading units.

Acknowledgements

Financial support for this work was provided by the Department of Chemical and Process Engineering at the University of Surrey and the EPSRC grant EP/R512904/1 as well as the Royal Society Research GrantRSGR1180353. LPP acknowledge Comunitat Valenciana for her APOSTD2017 fellowship. This work was also partially sponsored by the CO2Chem through the EPSRC grant EP/P026435/1.

References

[1] T.R. Knutson, R.E. Tuleya, Impact of CO_2-induced warming on simulated hurricane intensity and precipitation: sensitivity to the choice of climate model and convective parameterization, J. Clim. 17 (2004) 3477–3495.
[2] J. Hansen, M. Sato, R. Ruedy, K. Lo, D.W. Lea, M. Medina-Elizade, Global temperature change, Proc. Natl. Acad. Sci. 103 (2006) 14288–14293.
[3] X. Liu, C. Kunkel, P. Ramírez De La Piscina, N. Homs, F. Viñes, F. Illas, Effective and highly selective CO generation from CO_2 using a polycrystalline α-Mo_2C catalyst, ACS Catal. 7 (2017) 4323–4335.
[4] M.D. Porosoff, X. Yang, J.A. Boscoboinik, J.G. Chen, Molybdenum carbide as alternative catalysts to precious metals for highly selective reduction of CO_2 to CO, Angew. Chem. - Int. Ed. 53 (2014) 6705–6709.
[5] B. Lu, K. Kawamoto, Preparation of mesoporous CeO_2 and monodispersed NiO particles in CeO_2, and enhanced selectivity of NiO/CeO_2 for reverse water gas shift reaction, Mater. Res. Bull. 53 (2014) 70–78.
[6] C.S. Chen, W.H. Cheng, S.S. Lin, Mechanism of CO formation in reverse water–gas shift reaction over Cu/Al_2O_3 catalyst, Catal. Lett. 68 (2000) 45–48.
[7] S.S. Kim, H.H. Lee, S.C. Hong, A study on the effect of support's reducibility on the reverse water-gas shift reaction over Pt catalysts, Appl. Catal. A Gen. 423–424 (2012) 100–107.
[8] M.D. Porosoff, B. Yan, J.G. Chen, Catalytic reduction of CO_2 by H_2 for synthesis of CO, methanol and hydrocarbons: challenges and opportunities, Energy Environ. Sci. 9 (2016) 62–73.
[9] J. Li, L. Liu, Y. Liu, M. Li, Y. Zhu, H. Liu, Y. Kou, J. Zhang, Y. Han, D. Ma, Direct conversion of cellulose using carbon monoxide and water on a Pt–Mo_2C/C catalyst, Energy Environ. Sci. 7 (2014) 393–398.
[10] R.B. Levy, M. Boudart, Platinum-like behavior of tungsten carbide in surface catalysis, Science 181 (1973) 547–549.
[11] F. Viñes, J.A. Rodriguez, P. Liu, F. Illas, Catalyst size matters: tuning the molecular mechanism of the water-gas shift reaction on titanium carbide based compounds, J. Catal. 260 (2008) 103–112.
[12] P.M. Patterson, T.K. Das, B.H. Davis, Carbon monoxide hydrogenation over molybdenum and tungsten carbides, Appl. Catal. A Gen. 251 (2003) 449–455.
[13] C.I. Sathish, Y. Guo, X. Wang, Y. Tsujimoto, J. Li, S. Zhang, Y. Matsushita, Y. Shi, H. Tian, H. Yang, J. Li, K. Yamaura, Superconducting and structural properties of δ-MoC0.681cubic molybdenum carbide phase, J. Solid State Chem. 196 (2012) 579–585.
[14] H.W. Hugosson, P. Korzhavyi, U. Jansson, B. Johansson, O. Eriksson, Phase stabilities and structural relaxations in substoichiometric TiC1 − x, Phys. Rev. B - Condens. Matter Mater. Phys. 63 (2001) 1–8.
[15] W. Xu, P.J. Ramirez, D. Stacchiola, J.A. Rodriguez, Synthesis of α-MoC_{1-x} and β-MoC_y catalysts for CO_2 hydrogenation by thermal carburization of Mo-oxide in hydrocarbon and hydrogen mixtures, Catal. Lett. 144 (2014) 1418–1424.
[16] A. Goguet, F. Meunier, J.P. Breen, R. Burch, M.I. Petch, A. Faur Ghenciu, Study of the origin of the deactivation of a Pt/CeO_2 catalyst during reverse water gas shift (RWGS) reaction, J. Catal. 226 (2004) 382–392.
[17] F. Arena, G. Mezzatesta, G. Zafarana, G. Trunfio, F. Frusteri, L. Spadaro, Effects of oxide carriers on surface functionality and process performance of the Cu-ZnO system in the synthesis of methanol via CO_2 hydrogenation, J. Catal. 300 (2013) 141–151.
[18] H. Yue, Y. Zhao, S. Zhao, B. Wang, X. Ma, J. Gong, A copper-phyllosilicate core-sheath nanoreactor for carbon-oxygen hydrogenolysis reactions, Nat. Commun. 4 (2013) 1–7.
[19] X. Zhang, X. Zhu, L. Lin, S. Yao, M. Zhang, X. Liu, X. Wang, Y.W. Li, C. Shi, D. Ma, Highly dispersed copper over β-Mo_2C as an efficient and stable catalyst for the reverse water gas shift (RWGS) reaction, ACS Catal. 7 (2017) 912–918.
[20] P.S. Sai Prasad, J.W. Bae, K.W. Jun, K.W. Lee, Fischer-Tropsch synthesis by carbon dioxide hydrogenation on Fe-based catalysts, Catal. Surv. Asia 12 (2008) 170–183.
[21] C. Pistonesi, M.E. Pronsato, L. Bugyi, A. Juan, The adsorption of CO on potassium doped molybdenum carbide surface: an ab-initio study, Catal. Today 181 (2012) 102–107.
[22] H. Shou, D. Ferrari, D.G. Barton, C.W. Jones, R.J. Davis, Influence of passivation on the reactivity of unpromoted and Rb-promoted Mo2C nanoparticles for CO hydrogenation, ACS Catal. 2012 (2) (2012) 1408–1416.
[23] M.D. Porosoff, J.W. Baldwin, X. Peng, G. Mpourmpakis, H.D. Willauer, Potassium-promoted molybdenum carbide as a highly active and selective catalyst for CO_2 conversion to CO, ChemSusChem 10 (2017) 2408–2415.
[24] L. Pastor-Pérez, F. Baibars, E. Le Sache, H. Arellano-García, S. Gu, T.R. Reina, CO2 valorisation via reverse water-gas shift reaction using advanced Cs doped Fe-Cu/Al_2O_3 catalysts, J. CO_2 Util. 21 (2017) 423–428.
[25] C. Wan, Y.N. Regmi, B.M. Leonard, Multiple phases of molybdenum carbide as electrocatalysts for the hydrogen evolution reaction, Angew. Chemie - Int. Ed. 53 (2014) 6407–6410.
[26] P.K. Cheekatamarla, W.J. Thomson, Poisoning effect of thiophene on the catalytic activity of molybdenum carbide during tri-methyl pentane reforming for hydrogen generation, Appl. Catal. A Gen. 287 (2005) 176–182.
[27] J.G. Choi, L.T. Thompson, XPS study of as-prepared and reduced molybdenum oxides, Appl. Surf. Sci. 93 (1996) 143–149.
[28] L. Yang, W. Zhou, D. Hou, K. Zhou, G. Li, Z. Tang, L. Li, S. Chen, Porous metallic MoO2-supported MoS2 nanosheets for enhanced electrocatalytic activity in the hydrogen evolution reaction, Nanoscale 7 (2015) 5203–5208.
[29] K. Oshikawa, M. Nagai, S. Omi, Characterization of molybdenum carbides for methane reforming by TPR, XRD, and XPS, J. Phys. Chem. B 105 (2001) 9124–9131.
[30] Y. Ma, G. Guan, X. Hao, Z. Zuo, W. Huang, P. Phanthong, K. Kusakabe, A. Abudula, Highly-efficient steam reforming of methanol over copper modified molybdenum carbide, RSC Adv. 4 (2014) 44175–44184.
[31] C. Liu, M. Lin, D. Jiang, K. Fang, Y. Sun, Preparation of promoted molybdenum carbides nanowire for CO hydrogenation, Catal. Lett. 144 (2014) 567–573.
[32] E.T. Liakakou, E. Heracleous, Catalysis science & technology transition metal promoted K/Mo_2C as efficient catalysts for CO hydrogenation to higher alcohols, Catal. Sci. Technol. 6 (2015) 14–17.
[33] M. Lv, W. Xie, S. Sun, G. Wu, L. Zheng, S. Chu, C. Gao, J. Bao, Activated-carbon-supported K–Co–Mo catalysts for synthesis of higher alcohols from syngas, Catal. Sci. Technol. 5 (2015) 2925–2934.
[34] C. Liu, M. Lin, K. Fang, Y. Meng, Y. Sun, Preparation of nanostructured molybdenum carbides for CO hydrogenation, RSC Adv. 4 (2014) 20948–20954.
[35] J.A. Schaidle, A.C. Lausche, L.T. Thompson, Effects of sulfur on Mo_2C and Pt/Mo_2C catalysts: water gas shift reaction, J. Catal. 272 (2010) 235–245.
[36] P. Delporte, F. de´ric Meunier, C. Pham-Huu, P. Vennegues, M.J. Ledoux, J. Guille, Physical characterization of molybdenum oxycarbide catalyst; TEM, XRD and XPS, Catal. Today 23 (1995) 251–267.
[37] M. Bou, J.M. Martin, T. Le Mogne, L. Vovelle, Chemistry of the interface between aluminium and polyethyleneterephthalate by XPS, Appl. Surf. Sci. 47 (1991) 149–161.
[38] J. Ghijsen, L. Tjeng, J. van Elp, H. Eskes, J. Westerink, G. Sawatzky, M. Czyzyk, Electronic structure of Cu_2O and CuO, Phys. Rev. B 38 (1988) 11322–11330.
[39] NIST X-ray Photoelectron Spectroscopy Database, NIST Standard Reference Database Number 20, National Institute of Standards and Technology, Gaithersburg MD, 2000, p. 20899.
[40] M.T. Marques, A.M. Ferraria, J.B. Correia, A.M.B. Do Rego, R. Vilar, XRD, XPS and SEM characterisation of Cu-NbC nanocomposite produced by mechanical alloying, Mater. Chem. Phys. 109 (2008) 174–180.
[41] C.D. Wanger, W.M. Riggs, L.E. Davis, J.F. Moulder, G. E. Muilenberg Perkin-Elmer Corp, Handbook of X-Ray Photoelectron Spectroscopy, Perkin-Elmer Corporation, Physical Electronics Division, Eden Prairie, Minn, 1979, p. 55344.
[42] F. Parmigiani, G. Pacchioni, F. Illas, P.S. Bagus, Studies of the CuO bond in cupric oxide by X-ray photoelectron spectroscopy and ab-initio electronic structure models, J. Electron Spectros. Relat. Phenomena 59 (1992) 255–269.
[43] J. Jia, W. Zhou, Z. Wei, T. Xiong, G. Li, L. Zhao, X. Zhang, H. Liu, J. Zhou, S. Chen, Molybdenum carbide on hierarchical porous carbon synthesized from Cu-MoO2as efficient electrocatalysts for electrochemical hydrogen generation, Nano Energy 41 (2017) 749–757.
[44] X. Liu, Y. Song, W. Geng, H. Li, L. Xiao, W. Wu, Cu-Mo_2C/MCM-41: an efficient catalyst for the selective synthesis of methanol from CO2, Catalysts 6 (2016) 75.
[45] P. Xiao, Y. Yan, X. Ge, Z. Liu, J.Y. Wang, X. Wang, Investigation of molybdenum carbide nano-rod as an efficient and durable electrocatalyst for hydrogen evolution in acidic and alkaline media, Appl. Catal. B Environ. 154–155 (2014) 232–237.
[46] R. Kojima, K.I. Aika, Molybdenum nitride and carbide catalysts for ammonia synthesis, Appl. Catal. A Gen. 219 (2001) 141–147.
[47] M. Ghedira, M. Marezio, J. Mercier, The crystal structure of $Mo_{0.975}Ti_{0.025}O_2$ between 24 and 900°C, J. Solid State Chem. 59 (1985) 159–167.
[48] J.D. Hanawalt, H.W. Rinn, L.K. Frevel, Chemical analysis by X-Ray diffraction, Ind.

Eng. Chem. Anal. Ed. 10 (1938) 457–512.
[49] Y. Luo, Z. Wang, Y. Fu, C. Jin, Q. Wei, R. Yang, In situ preparation of hollow Mo_2C–C hybrid microspheres as bifunctional electrocatalysts for oxygen reduction and evolution reactions, J. Mater. Chem. A Mater. Energy Sustain. 4 (2016) 12583–12590.
[50] J. Chen, W. Zhou, J. Jia, B. Wan, J. Lu, T. Xiong, Q. Tong, S. Chen, Porous molybdenum carbide microspheres as efficient binder-free electrocatalysts for suspended hydrogen evolution reaction, Int. J. Hydrogen Energy 42 (2017) 6448–6454.
[51] P. Gao, F. Li, F. Xiao, N. Zhao, W. Wei, L. Zhong, Y. Sun, Effect of hydrotalcite-containing precursors on the performance of Cu/Zn/Al/Zr catalysts for CO_2hydrogenation: Introduction of Cu^{2+} at different formation stages of precursors, Catal. Today 194 (2012) 9–15.
[52] W. Wu, Z. Wu, C. Liang, P. Ying, Z. Feng, C. Li, An IR study on the surface passivation of Mo_2C/Al_2O_3 catalyst with O_2, H_2O and CO_2, Phys. Chem. Chem. Phys. 6 (2004) 5603–5608.
[53] M. Nagai, T. Kurakami, S. Omi, Activity of carbided molybdena ± alumina for CO_2 hydrogenation, Catal. Today 45 (1998) 235–239.
[54] H. Shou, D. Ferrari, D.G. Barton, C.W. Jones, R.J. Davis, Influence of Passivation on the reactivity of unpromoted and Rb-promoted Mo2C nanoparticles for CO hydrogenation, ACS Catal. 2 (2012) 1408–1416.
[55] J. Gao, Y. Wu, C. Jia, Z. Zhong, F. Gao, Y. Yang, B. Liu, Controllable synthesis of α-MoC_{1-x} and β-Mo_2C nanowires for highly selective CO_2 reduction to CO, Catal. Commun. 84 (2016) 147–150.